SOBEL-LBP

Sanqiang Zhao[1], Yongsheng Gao[1], and Baochang Zhang[1,2]
[1]School of Engineering, Griffith University, Nathan Campus, QLD 4111, Australia
[2]School of Automation Science and Electrical Engineering, Beihang University, Beijing 100083, China
{s.zhao, yongsheng.gao, b.zhang}@griffith.edu.au

ABSTRACT

This paper presents a new Sobel-LBP, an extension of existing Local Binary Pattern (LBP), for facial image representation. The face image is filtered by Sobel operator to enhance the edge information. Sobel-LBP feature distributions are then extracted and concatenated into a spatial histogram to be used as a face descriptor. The proposed method is compared with the original LBP on both gray-level images and Gabor real and imaginary features for face recognition. The experimental results indicate that Sobel-LBP provides a significantly better performance than LBP under various conditions.

Index Terms—Image representation, face recognition, Local Binary Pattern, Sobel-LBP, Gabor feature

1. INTRODUCTION

The large number of emerging applications and the growing interest in computer vision systems have fueled the need of efficient algorithms to cope with numerous challenges associated in face analysis. A key issue in face analysis is to find a discriminative and efficient representation for face images. Many holistic methods such as Principal Component Analysis (PCA) [1] and Linear Discriminant Analysis (LDA) [2] have been widely investigated due to their effectiveness to capture the variance in the training database. Two well-known face recognition methods, Eigenface and Fisherface built on the above two techniques respectively, have been proved successful.

Meanwhile, local methods have also gained much attention in the face recognition community due to their robustness to illumination and pose variations. In Local Feature Analysis (LFA) [3], a dense set of local-topological fields are developed to extract local features. Based on Gabor features, Elastic Bunch Graph Matching (EBGM) [4] achieved a noticeable performance in the FERET evaluation test [5]. The recently proposed Local Binary Pattern (LBP) approach [6] has evolved to represent a significant breakthrough in face representation, outperforming earlier methods such as PCA, LDA and EBGM [7]. The idea behind using the LBP features is that a face can be seen as a composition of micro-patterns generated by the concatenation of the circular binary gradients. Two most important properties of the LBP operator in real-world applications are its computational simplicity and tolerance against illumination changes. The first property makes it possible to analyze images in challenging real-time settings. The LBP operator has been successfully applied to texture analysis [6], facial expression analysis [8] and background modeling [9].

In this paper, we propose a new Sobel-LBP, which is an extension of the LBP operator. We argue that the performance of LBP can be greatly improved through Sobel operator prior to feature extraction. As LBP extracts the circular binary gradients at a micro-level, Sobel operator provides the function of enhancing this gradient information accordingly. Compared with LBP, Sobel-LBP achieves superior performance in our comparative experiments. Besides, we extend Sobel-LBP to Gabor features. It is demonstrated that Sobel-LBP outperforms LBP on both Gabor real and imaginary features, which can effectively enhance the recognition performance of the proposed Sobel-LBP method. Different from the learning-based methods, Sobel-LBP is directly extracted from images or Gabor features without any training procedure, and thus is applicable to the systems where only one sample image per person is available. Similar to but better than LBP, Sobel-LBP is a micro-pattern presented in a general form which can capture more gradient information from local variances. Due to its micro-pattern representation, Sobel-LBP is also modeled by histogram to preserve the information about its distribution.

The rest of this paper is organized as follows. Section 2 presents the proposed Sobel-LBP in detail. Section 3 applies Sobel-LBP to Gabor real and imaginary features. In Section 4, comparative experiments on FERET database [5] are conducted to evaluate the performance of Sobel-LBP on face recognition. The last section concludes the paper.

2. SOBEL-LBP

In this section, we first provide a brief introduction of Local Binary Pattern (LBP), and then describe Sobel-LBP in detail. The procedure of constructing the spatial histogram is followed to model the distribution of Sobel-LBP for face representation.

2.1. Local Binary Pattern

Initially derived from texture analysis community, the LBP operator was created as a gray-level invariant texture measure to model texture images [6]. Later, it demonstrated excellent performance in many other research fields in terms of both speed and discrimination capability [7, 8, 9]. Mathematically, it marks each pixel I_c of an image as a decimal number $LBP_{P,R}(I_c)$, which is formed by thresholding the P equally spaced neighbor pixels $I_{p,R}$ $(p=0,\cdots,P-1)$ on a circle of radius R with the center pixel I_c and concatenating the results binomially with factor 2^p:

$$LBP_{P,R}=\sum_{p=0}^{P-1}s\left(I_{p,R}-I_c\right)2^p, \tag{1}$$

where the thresholding function $s(x)$ is defined as

$$s\left(x\right)=\begin{cases}1, & x\geq 0\\ 0, & x<0\end{cases}. \tag{2}$$

If the coordinate of I_c is $(0,\ 0)$, the coordinates of $I_{p,R}$ are given by $(-R\sin(2\pi p/P),\ R\cos(2\pi p/P))$. The gray-level values of neighbors $I_{p,R}$ not falling exactly in the center of pixels are estimated by interpolation [6]. Fig. 1 illustrates an example of obtaining a LBP micro-pattern $LBP_{8,1}$ with the parameters $P=8$ and $R=1$.

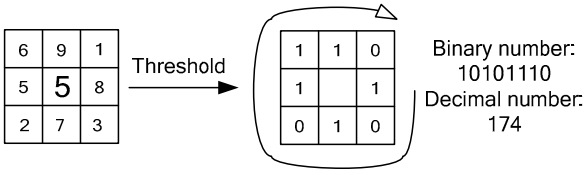

Fig. 1. LBP operator.

2.2. Sobel-LBP

LBP actually encodes the micro-level information of edges, spots and other local features in an image. Based on this observation, we argue that combining Sobel operator with LBP can enhance the local features, and thus more detailed information can be extracted from LBP operation. This new operator is named as Sobel-LBP. Because Sobel operator is very easy and efficient to implement, it only slightly increases the computational work of LBP feature extraction process.

The Sobel operator contains two 3×3 kernels (horizontal kernel S_x and vertical kernel S_y) which are convolved with the original image I to calculate gradient approximations:

$$I^x=S_x*I=\begin{bmatrix}1 & 0 & -1\\ 2 & 0 & -2\\ 1 & 0 & -1\end{bmatrix}*I,\ I^y=S_y*I=\begin{bmatrix}1 & 2 & 1\\ 0 & 0 & 0\\ -1 & -2 & -1\end{bmatrix}*I, \tag{3}$$

where I^x and I^y represent the horizontally and vertically filtered results, respectively. Normally I^x and I^y are combined to give the gradient magnitude $\sqrt{(I^x)^2+(I^y)^2}$. Here the Sobel-LBP operator is defined as the concatenation of LBP operations on I^x and I^y:

$$Sobel\text{-}LBP_{P,R}=\left\{Sobel\text{-}LBP^x_{P,R},\ Sobel\text{-}LBP^y_{P,R}\right\}, \tag{4}$$

where

$$\begin{aligned}Sobel\text{-}LBP^x_{P,R}&=\sum_{p=0}^{P-1}s\left(I^x_{p,R}-I^x_c\right)2^p\\ Sobel\text{-}LBP^y_{P,R}&=\sum_{p=0}^{P-1}s\left(I^y_{p,R}-I^y_c\right)2^p\end{aligned}. \tag{5}$$

2.3. Histogram of Sobel-LBP

The histograms of the Sobel-LBP micro-patterns contain the distribution information of the local features in an image. In order to preserve spatial information, a face image is divided into several non-overlapping rectangular sub-regions. Fig. 2 illustrates an example of face image divided into 3×3 sub-regions. A spatial histogram, which concatenates the histograms of all the sub-regions, is employed to represent the face. The spatial histogram encodes both the appearance and the spatial relations of facial regions. Let $H_{Sobel\text{-}LBP}(R_i)$ denote the histogram of the Sobel-LBP patterns extracted from the sub-region R_i $(i=1,\cdots,N)$. The spatial histogram of the face image is represented as

$$SH\left(I\right)=\left\{H_{Sobel\text{-}LBP}\left(R_i\right)\,|\,i=1,\cdots,N\right\}. \tag{6}$$

Note the sub-regions can be of different shapes other than rectangles, of different sizes, or partially overlapping.

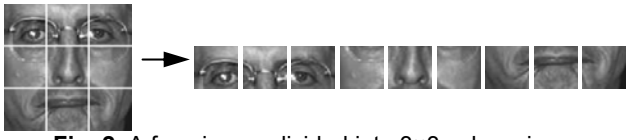

Fig. 2. A face image divided into 3×3 sub-regions.

There are many similarity measures for histogram matching. In this paper, histogram intersection is utilized to compare two spatial histograms SH^1 and SH^2:

$$S_{HI}\left(SH^1,SH^2\right)=\sum_{i,j}\min\left(SH^1_{i,j},SH^2_{i,j}\right), \tag{7}$$

where indices i and j refer to j^{th} bin in histogram corresponding to the i^{th} sub-region. This measure has an intuitive motivation in that it calculates the common parts of two histograms. Because it requires only simple operations, its computational complexity is very low.

3. SOBEL-LBP ON GABOR FEATURES

In image processing and object recognition, one of the widely used image feature descriptors is Gabor features. They can capture the salient visual properties in an image,

such as spatial characteristics, because the kernels can selectively enhance features in certain scales and orientations. LBP operator has been successfully applied on both Gabor magnitudes [10] and Gabor phases [11]. In this section, we also extend Sobel-LBP operator from spatial domain to Gabor feature domain. Different from [10] and [11], we apply Sobel-LBP to Gabor real features and imaginary features. It is demonstrated that both Gabor real and imaginary features are able to enhance the object representation capability. Still, Sobel-LBP outperforms LBP on both feature domains. The 2D Gabor kernel functions used for feature extraction are

$$\psi_j(\mathbf{z}) = \frac{k_j^2}{\sigma^2}\exp\left(-\frac{k_j^2 z^2}{2\sigma^2}\right)\left[\exp\left(i\mathbf{k_j z}\right) - \exp\left(-\frac{\sigma^2}{2}\right)\right], \quad (8)$$

where

$$\mathbf{k_j} = \begin{pmatrix} k_{jx} \\ k_{jy} \end{pmatrix} = \begin{pmatrix} k_\nu \cos\varphi_\mu \\ k_\nu \sin\varphi_\mu \end{pmatrix}, \ k_\nu = 2^{-\frac{\nu+2}{2}}\pi, \ \varphi_\mu = \mu\frac{\pi}{8}. \quad (9)$$

The index $j = \mu + 8\nu$ covers a discrete set of five different frequencies $\nu = 0,\cdots,4$ and eight orientations $\mu = 0,\cdots,7$. The width of the Gaussian is controlled by the parameter $\sigma = 2\pi$ [4, 12]. The Gabor features $G_j(\mathbf{z})$ of a given image $I(\mathbf{z})$ are defined as its convolution with 40 Gabor kernels:

$$G_j(\mathbf{z}) = I(\mathbf{z}) * \psi_j(\mathbf{z}). \quad (10)$$

An example of Gabor real and imaginary features is illustrated in Fig. 3.

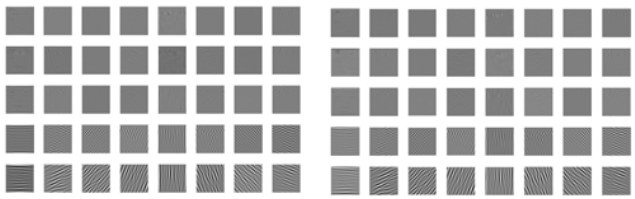

(a) (b)

Fig. 3. Gabor features. (a) Real part. (b) Imaginary part.

Let G_j^{Re} and G_j^{Im} denote the Gabor real and imaginary features of an image, respectively, where $j = 0,\cdots,39$. The Gabor real and imaginary Sobel-LBPs can be defined as

$$G\_Sobel\text{-}LBP_{j,P,R}^{\mathrm{Re}} = \{\sum_{p=0}^{P-1} s\left(S_x * G_{j,p,R}^{\mathrm{Re}} - S_x * G_{j,c}^{\mathrm{Re}}\right)2^p, \sum_{p=0}^{P-1} s\left(S_y * G_{j,p,R}^{\mathrm{Re}} - S_y * G_{j,c}^{\mathrm{Re}}\right)2^p\}, \quad (11)$$

$$G\_Sobel\text{-}LBP_{j,P,R}^{\mathrm{Im}} = \{\sum_{p=0}^{P-1} s\left(S_x * G_{j,p,R}^{\mathrm{Im}} - S_x * G_{j,c}^{\mathrm{Im}}\right)2^p, \sum_{p=0}^{P-1} s\left(S_y * G_{j,p,R}^{\mathrm{Im}} - S_y * G_{j,c}^{\mathrm{Im}}\right)2^p\}. \quad (12)$$

Similar to modeling the image Sobel-LBP, the spatial histograms of Gabor real and imaginary Sobel-LBPs are represented as

$$SHG^{\mathrm{Re}}(I) = \left\{H_{G\_Sobel\text{-}LBP_j^{\mathrm{Re}}}(R_i) \mid i = 1,\cdots,N; j = 0,\cdots,39\right\}, \quad (13)$$

$$SHG^{\mathrm{Im}}(I) = \left\{H_{G\_Sobel\text{-}LBP_j^{\mathrm{Im}}}(R_i) \mid i = 1,\cdots,N; j = 0,\cdots,39\right\}. \quad (14)$$

It should be noted that Sobel-LBP extracted from Gabor features induces a high dimensionality of the histogram vector (40 times longer than that of image Sobel-LBP). To alleviate this problem, the uniform quantization method is utilized to partition the sub-region histogram with equal intervals. If the number of the histogram bins in each sub-region is defined as B, then these B bins with equal size $256/B$ can be represented as $[0,\cdots,256/B-1]$, $[256/B,\cdots,2\times 256/B-1]$, $\cdots$, $[(B-1)\times 256/B,\cdots,255]$. The selection of an optimal number of histogram bins is a compromise between recognition performance and speed.

4. EXPERIMENTAL RESULTS

The proposed Sobel-LBP method is assessed on the publicly available FERET database [5]. All the images are normalized and cropped to 88×88 pixels based on the positions of two eyes provided within the FERET database. The experiments are divided into two parts. Experiment A reports the results of Sobel-LBP on gray-level images, and Experiment B presents the results of Sobel-LBP on Gabor features. In both experiments, we compare the Sobel-LBP operator and the LBP operator using the same radius and sampling points ($P = 8$, $R = 1$), with varying sub-region divisions and different sub-region histogram bins.

Experiment A: Sobel-LBP on Images

To observe the performance of Sobel-LBP under different conditions, the experiments are first conducted on the original images from individual probe sets against the gallery set FA. Fig. 4 illustrates the recognition accuracy of both Sobel-LBP and LBP on four probe sets with the same sub-region size of 4×4 pixels. Two different numbers of histogram bins (16 and 32) in each sub-region are tested. It can be seen from the chart that an increasing number of histogram bins improves the recognition rates of both Sobel-LBP and LBP. But Sobel-LBP outperforms LBP on both two numbers of histogram bins with only one exception of FB probe set, where Sobel-LBP performs slightly inferior to LBP. This could be caused by the fact that Sobel-LBP is sensitive to expression variations to a certain extent. It is interesting to note that when the test images are of significant detrimental quality (FC and Dup II), Sobel-LBP demonstrates a significantly better performance than LBP.

We also use the same number (32) of histogram bins, and examine the influence of different sub-region sizes on the recognition rates. Fig. 5 demonstrates that when the sub-region size increases, the overall system performance degrades accordingly due to the loss of spatial information. This indicates a trade-off between the system performance and the feature size. In Fig. 5(a), Sobel-LBP noticeably improves the average recognition rate of LBP by 35.2%.

Experiment B: Sobel-LBP on Gabor Features

The experiments are also designed on Gabor features. Fig. 6 displays the effectiveness of Gabor Sobel-LBP (G_Sobel-LBP) on face recognition. For a fair comparison, LBP is also extracted from Gabor real and imaginary features, named Gabor LBP (G_LBP). In this experiment, we fix the parameters to 11×11-sized sub-regions and 32 histogram bins. It can be induced from Fig. 6 that Gabor Sobel-LBP and Gabor LBP have achieved better performances than image Sobel-LBP and image LBP respectively, which confirms that Sobel-LBP and LBP are both effective on Gabor real and imaginary features. The performance of Gabor real features is comparable to that of Gabor imaginary features. It should be noted that Gabor Sobel-LBP performs consistently better than Gabor LBP over all the probe sets.

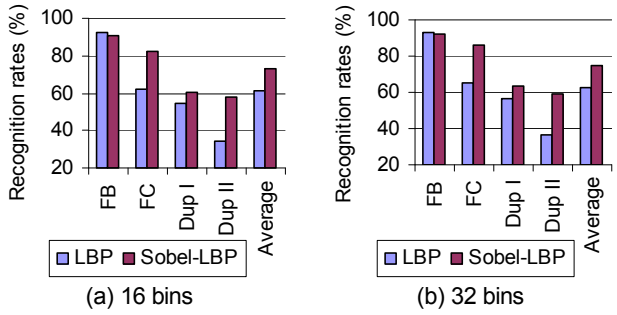

Fig. 4. Comparative recognition rates on images with 4×4-sized sub-regions.

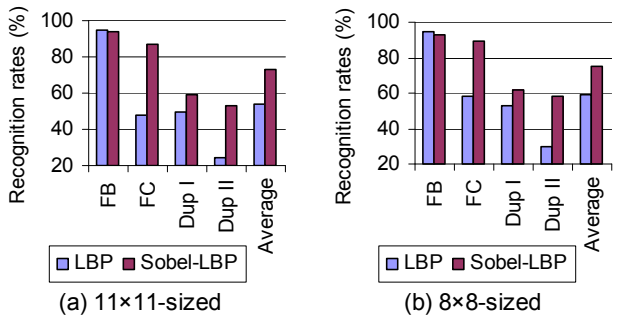

Fig. 5. Comparative recognition rates on images with 32 histogram bins.

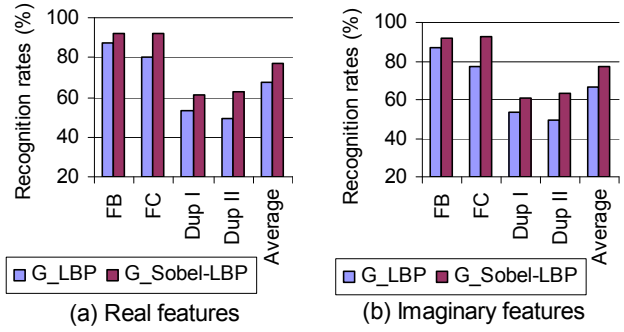

Fig. 6. Comparative recognition rates on Gabor features with 11×11-sized sub-regions and 32 histogram bins.

5. CONCLUSIONS

This paper extends existing Local Binary Pattern (LBP) and presents a new operator, Sobel-LBP, for facial image description and recognition. The feasibility and effectiveness of using this operator is investigated. We used FERET database to conduct comparative experiments between LBP and Sobel-LBP on both gray-level images and Gabor real and imaginary features. The results demonstrate that Sobel-LBP significantly outperforms LBP with various parameters including different sub-region divisions and different sub-region histogram bins, under various conditions including different illuminations and different time.

6. ACKNOWLEDGEMENT

This research was supported by the Australian Research Council (ARC) Discovery Grants DP0451091 and DP0877929.

7. REFERENCES

[1] M.A. Turk and A.P. Pentland, "Face Recognition Using Eigenfaces," *Proceedings of CVPR*, pp. 586-591, 1991.

[2] P.N. Belhumeur, J.P. Hespanha, and D.J. Kriegman, "Eigenfaces vs. Fisherfaces: Recognition Using Class Specific Linear Projection," *TPAMI*, vol. 19, pp. 711-720, 1997.

[3] P.S. Penev and J.J. Atick, "Local Feature Analysis: A General Statistical Theory for Object Representation," *Network: Computation in Neural Systems*, vol. 7, pp. 477-500, 1996.

[4] L. Wiskott, J.M. Fellous, N. Krüger, and C. von der Malsburg, "Face Recognition by Elastic Bunch Graph Matching," *TPAMI*, vol. 19, pp. 775-779, 1997.

[5] P.J. Phillips, H. Moon, S.A. Rizvi, and P.J. Rauss, "The FERET Evaluation Methodology for Face-Recognition Algorithms," *TPAMI*, vol. 22, pp. 1090-1104, 2000.

[6] T. Ojala, M. Pietikäinen, and T. Mäenpää, "Multiresolution Gray-Scale and Rotation Invariant Texture Classification with Local Binary Patterns," *TPAMI*, vol. 24, pp. 971-987, 2002.

[7] T. Ahonen, A. Hadid, and M. Pietikäinen, "Face Description with Local Binary Patterns: Application to Face Recognition," *TPAMI*, vol. 28, pp. 2037-2041, 2006.

[8] G. Zhao and M. Pietikäinen, "Dynamic Texture Recognition Using Local Binary Patterns with an Application to Facial Expressions," *TPAMI*, vol. 29, pp. 915-928, 2007.

[9] M. Heikkilä and M. Pietikäinen, "A Texture-Based Method for Modeling the Background and Detecting Moving Objects," *TPAMI*, vol. 28, pp. 657-662, 2006.

[10] W. Zhang, S. Shan, W. Gao, X. Chen, and H. Zhang, "Local Gabor Binary Pattern Histogram Sequence (LGBPHS): A Novel Non-Statistical Model for Face Representation and Recognition," *Proceedings of ICCV*, pp. 786-791, 2005.

[11] B. Zhang, S. Shan, X. Chen, and W. Gao, "Histogram of Gabor Phase Patterns (HGPP): A Novel Object Representation Approach for Face Recognition," *IEEE Transactions on Image Processing*, vol. 16, pp. 57-68, 2007.

[12] S. Zhao, W. Gao, S. Shan, and B. Yin, "Enhance the Alignment Accuracy of Active Shape Models Using Elastic Graph Matching," *Proceedings of ICBA*, pp. 52-58, 2004.